

Technical Report for Planar Domain Parameterization Based on Quasi-conformal Mapping

Maodong Pan^{a,b,1,*}, Yinlei Hu^b, Yuanpeng Zhu^c

^a*Institute of Applied Geometry, Johannes Kepler University Linz, Altenberger Str.69, 4040 Linz, Austria*

^b*School of Mathematical Sciences, University of Science and Technology of China, Hefei 230026, PR China*

^c*School of Mathematics, South China University of Technology, Guangzhou 510641, PR China*

Abstract

This technical report is a supplementary document of our work [1] for the planar domain parameterization based on quasi-conformal mapping, in which the detailed discussions on **the initial construction of the parameterization** and two sub-problems involved in the optimization model (7) are presented, the comparisons with Teichmüller map (T-Map) method [2] in terms of angle distortion and area distortion are provided, at the same time, some numerical examples in the subsequent simulation of isogeometric analysis are also demonstrated to show the advantages of our method than previous approaches [2, 3].

1. Initialization of the parameterization

A good initialization method is critical for reducing the number of iterations in the optimization procedure. In this paper, we study and compare two sets of initialization methods: Coons patch based and harmonic mapping based methods.

1.1. Coons patch interpolation

Given the boundary control points $\mathbf{c}_{0j}, \mathbf{c}_{mj}, \mathbf{c}_{i0}, \mathbf{c}_{in}, i = 0, \dots, m, j = 0, \dots, n$ of the parameterization, the inner control points $\mathbf{c}_{ij} (i = 1, \dots, m-1, j = 1, \dots, n-1)$ can be constructed by coons patch interpolation method as follows

$$\begin{aligned} \mathbf{c}_{ij} = & \left(1 - \frac{i}{m}\right) \mathbf{c}_{0j} + \frac{i}{m} \mathbf{c}_{mj} + \left(1 - \frac{j}{n}\right) \mathbf{c}_{i0} + \frac{j}{n} \mathbf{c}_{in} \\ & - \left[\begin{array}{cc} 1 - \frac{i}{m} & \frac{i}{m} \end{array} \right] \left[\begin{array}{cc} \mathbf{c}_{00} & \mathbf{c}_{0n} \\ \mathbf{c}_{m0} & \mathbf{c}_{mn} \end{array} \right] \left[\begin{array}{c} 1 - \frac{j}{n} \\ \frac{j}{n} \end{array} \right]. \end{aligned}$$

1.2. Harmonic mapping based method

The second type of initialization method is through harmonic mapping, which is used in this work. According to the smooth harmonic map theory, a harmonic map f is a function satisfying Laplace's equation, i.e., $f_{z\bar{z}} = 0$.

*Corresponding author.

Email address: mdpan@mail.ustc.edu.cn, maodong.pan@jku.at (Maodong Pan)

¹This work was done while this author was with University of Science and Technology of China, and now he is working at Johannes Kepler University Linz.

Model	Convergence time (s)	
	Coons interpolation	Harmonic mapping
Bird		
Cow		
Tree		
Vase		
China Map		
Rabbit		

Table 1:

2. Two subproblems involved in the optimization model (7)

τ -subproblem Given the map f from $\hat{\Omega}$ to Ω , from the equation (1) in Definition 1, the Beltrami coefficient of f can be computed as

$$\mu(f) = \frac{f_z}{f_z} = \frac{f_\xi + i f_\eta}{f_\xi - i f_\eta} = \frac{(a - b) + \sqrt{-1}(c + d)}{(a + b) + \sqrt{-1}(c - d)}$$

where

$$\begin{aligned} a &= \sum_{i=0}^m \sum_{j=0}^n c_{ij}^x \frac{\partial N_i^p(\xi)}{\partial \xi} N_j^q(\eta), & b &= \sum_{i=0}^m \sum_{j=0}^n c_{ij}^y N_i^p(\xi) \frac{\partial N_j^q(\eta)}{\partial \eta}, \\ c &= \sum_{i=0}^m \sum_{j=0}^n c_{ij}^y \frac{\partial N_i^p(\xi)}{\partial \xi} N_j^q(\eta), & d &= \sum_{i=0}^m \sum_{j=0}^n c_{ij}^x N_i^p(\xi) \frac{\partial N_j^q(\eta)}{\partial \eta}. \end{aligned}$$

Then the subproblem for τ in problem (7) is equal to the following model:

$$\begin{aligned} \arg \min_{\tau} & \int_{\hat{\Omega}} |\tau|^2 dz + \beta \int_{\hat{\Omega}} |\tau - \mu(f)|^2 dz \\ \text{s.t. } & \sup_{z \in \hat{\Omega}} |\tau| < 1. \end{aligned} \tag{8}$$

Assume

$$\tau = \sum_{i=0}^m \sum_{j=0}^n (\hat{c}_{ij}^x + \sqrt{-1} \hat{c}_{ij}^y) N_i^p(\xi) N_j^q(\eta), \tag{9}$$

where $N_i^p(\xi)$ and $N_j^q(\eta)$ are B-spline basis functions defined in Section 2.2. For the simplicity of computation, we replace the constraint $\sup_{z \in \hat{\Omega}} |\tau| < 1$ in the above optimization problem with

$$-\frac{\sqrt{2}}{2} < \hat{c}_{ij}^x < \frac{\sqrt{2}}{2}, \quad -\frac{\sqrt{2}}{2} < \hat{c}_{ij}^y < \frac{\sqrt{2}}{2}, \quad i = 0, 1, \dots, m, j = 0, 1, \dots, n \tag{10}$$

so the problem (8) is relaxed as the following quadratic optimization problem:

$$\begin{aligned} \arg \min_{\hat{c}_{ij}^x, \hat{c}_{ij}^y} & \int_{\hat{\Omega}} |\tau|^2 dz + \beta \int_{\hat{\Omega}} |\tau - \mu(f)|^2 dz \\ \text{s.t. } & -\frac{\sqrt{2}}{2} < \hat{c}_{ij}^x < \frac{\sqrt{2}}{2}, \quad -\frac{\sqrt{2}}{2} < \hat{c}_{ij}^y < \frac{\sqrt{2}}{2}, \quad i = 0, 1, \dots, m, j = 0, 1, \dots, n. \end{aligned} \tag{11}$$

which can be easily solved by the interior-point method, and the solution must exist.

f -subproblem Given τ , the subproblem for f in problem (7) reduces to the following model:

$$\begin{aligned} & \arg \min_{c_{ij}^x, c_{ij}^y} \alpha \int_{\hat{\Omega}} D_{fair}(f; z) dz + \beta \int_{\hat{\Omega}} |\tau - \mu(f)|^2 dz \\ & \text{s.t. } f|_{\partial\hat{\Omega}} \text{ is given.} \end{aligned} \quad (12)$$

However, since $\mu(f) = f_{\bar{z}}/f_z$ is a rational B-spline function and the constraints in (12) are hard, the problem is still difficult to solve. Instead we solve the following relaxed unconstrained model:

$$\arg \min_{c_{ij}^x, c_{ij}^y} \alpha \int_{\hat{\Omega}} D_{fair}(f; z) dz + \beta \int_{\hat{\Omega}} |\tau f_z - f_{\bar{z}}|^2 dz + \gamma \|\Theta(C) - \theta\|^2 \quad (13)$$

where γ is a large positive weight, C is the complex coefficient matrix, $\theta \in \mathbb{C}^{2(m+n)}$ is the vector of observations (i.e., boundary control points of the parameterization f) and $\Theta : \mathbb{C}^{(m+1) \times (n+1)} \rightarrow \mathbb{C}^{2(m+n)}$ is a linear operator that shapes the prespecified elements of C into a vector. Note that the rational function $\int_{\hat{\Omega}} |\tau - \mu(f)|^2 dz$ in (12) is subtly converted into the quadratic term $\int_{\hat{\Omega}} |\tau f_z - f_{\bar{z}}|^2 dz$ in (13). It is easy to see that (13) is a quadratic optimization problem and the solution can be obtained by solving a sparse and symmetric linear system of equations. The preconditioned conjugate gradient method with incomplete Cholesky factorization is applied in our algorithm.

Now the overall algorithm of our method is summarized in Algorithm 1.

Algorithm 1 The parameterization algorithm based on quasi-conformal mapping

Input:

B-spline representations of four boundary curves of the domain Ω , $\alpha, \beta, \gamma, \epsilon$

Output:

A quasi-conformal map f from the unit square $\hat{\Omega}$ to Ω

- 1: $n = 0$
 - 2: Compute an approximate harmonic map f_0 by solving the optimization problem (4)
 - 3: **repeat**
 - 4: Fixing f_n , minimize (8) to obtain τ_n
 - 5: Fixing τ_n , minimize (12) obtain f_{n+1}
 - 6: $n \leftarrow n + 1$
 - 7: **until** $\|\tau_{n+1} - \tau_n\|_\infty < \epsilon$
-

Remark 1. The proposed parameterization model (5) is non-linear and non-convex, and it is in general hard to solve. Instead we solve the problem using an energy descent method, which solves two quadratic problems alternatively and converges to a stationary point [4, 5]. And in each iteration, there exists a local minimizer for each of the quadratic problems. However, we are not able to prove that a minimizer of the parameterization model (5) is guaranteed to exist, even though in practice our model works well for producing high-quality parameterizations for general domains (even complicated domains).

3. Parameterization quality

In this part, six parameterization examples are presented to show the effectiveness of the proposed method. The comparisons with Teichmuller map (T-Map) method [2] in terms of conformal distortion and area distortion are also provided.

Fig. 1 illustrates the conformal distortion of the parameterization by the T-Map method and our method. Obviously we can see that the T-Map method is significantly worse than our method in terms of the conformal distortion. In Fig. 2, we compare our method with T-Map method by displaying the area distortion. It can be seen that our method produces much lower distortion in some concave regions. More results with complex geometries for our approach are also demonstrated in Fig. 3, including the vase mode, China map model and rabbit model.

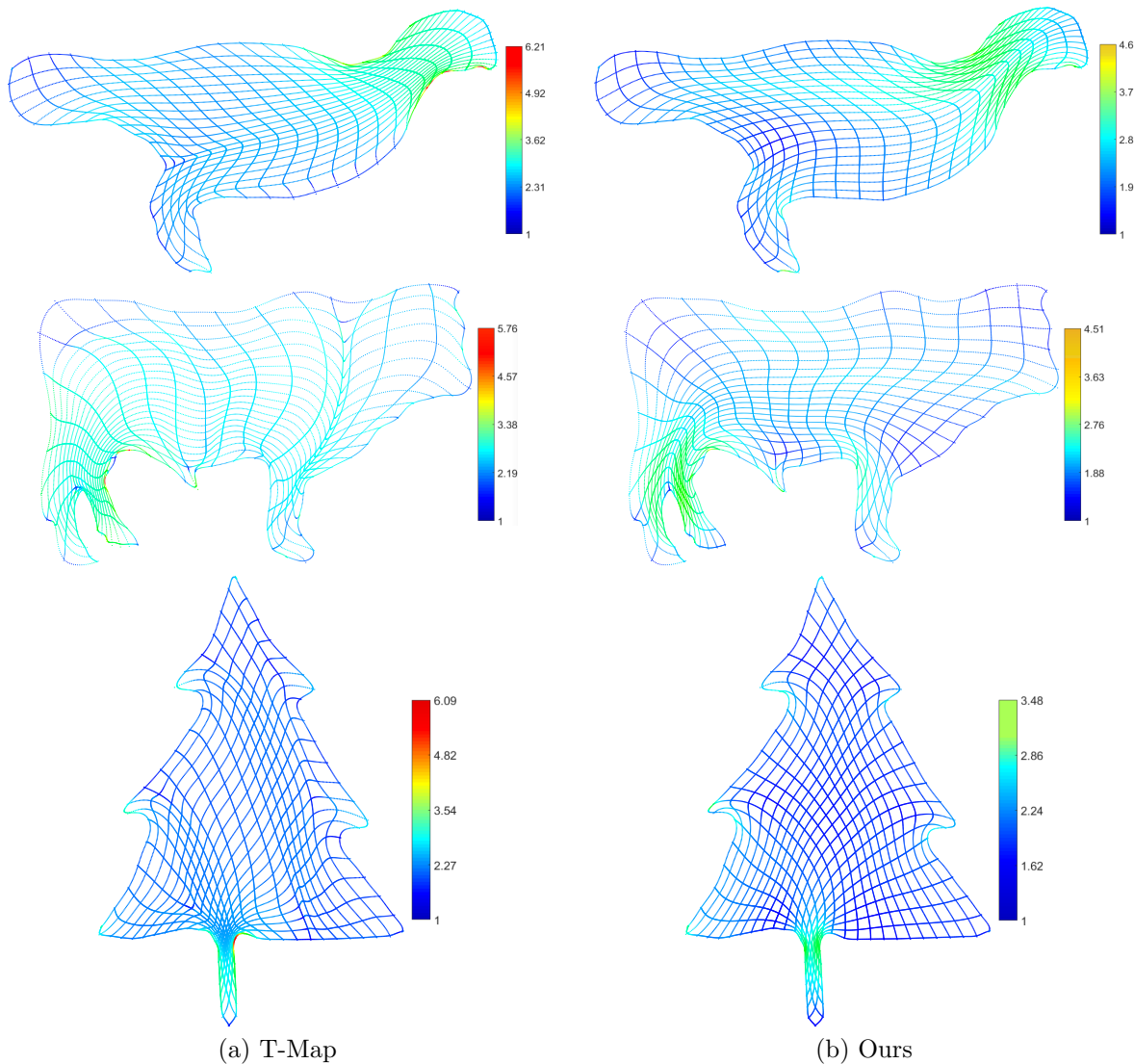


Figure 1: Conformal (angle) distortion of the parameterization results by different methods: (a) Teichmüller mapping method and (b) Our method. Each sub-figure shows the colormaps of $\log_2 \kappa(J_f)$.

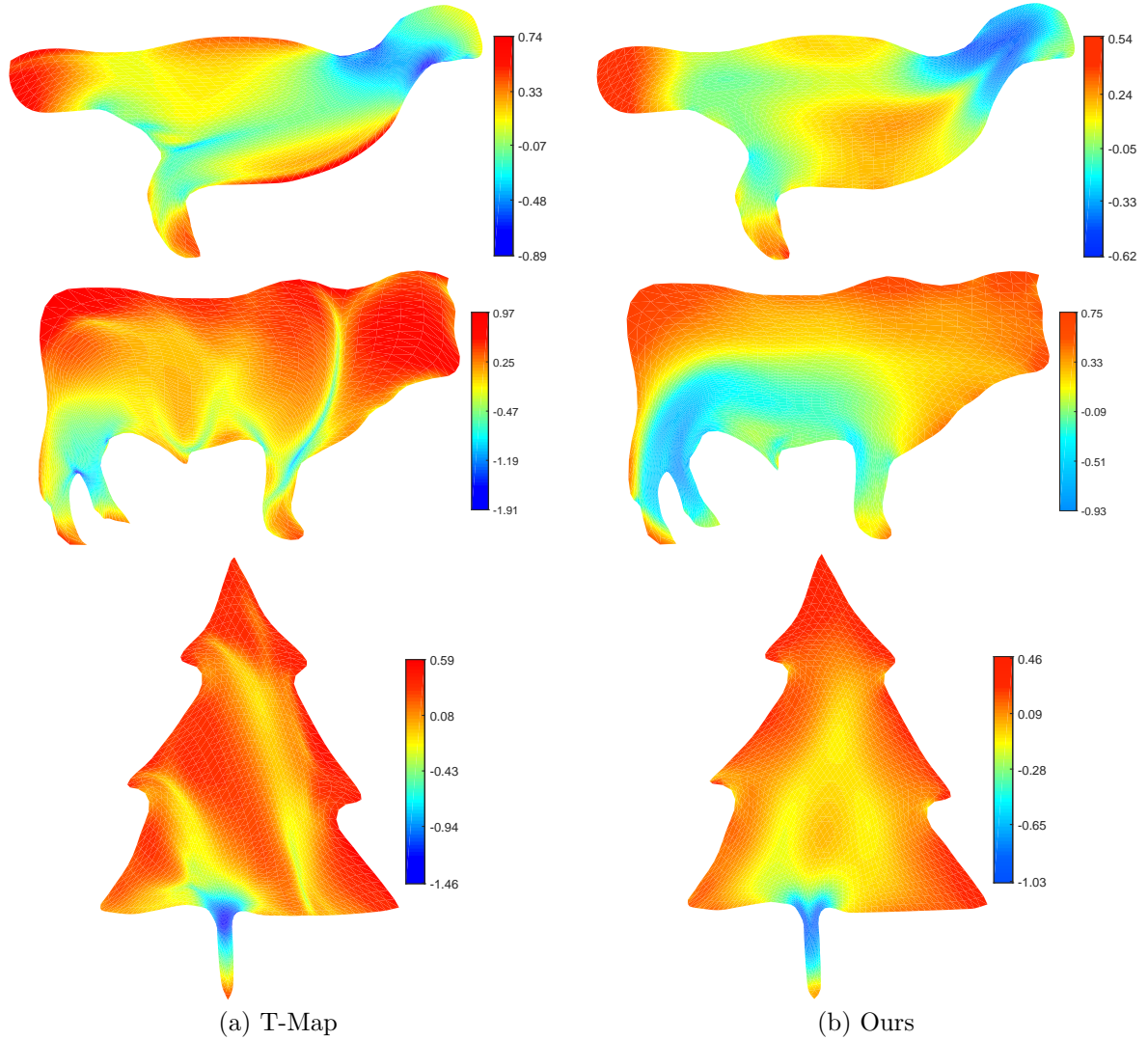


Figure 2: Area distortion of the parameterization results by different methods: (a) Teichmüller mapping method and (b) Our method. Each sub-figure shows the colormaps of $\log_{10} J_f^s$.

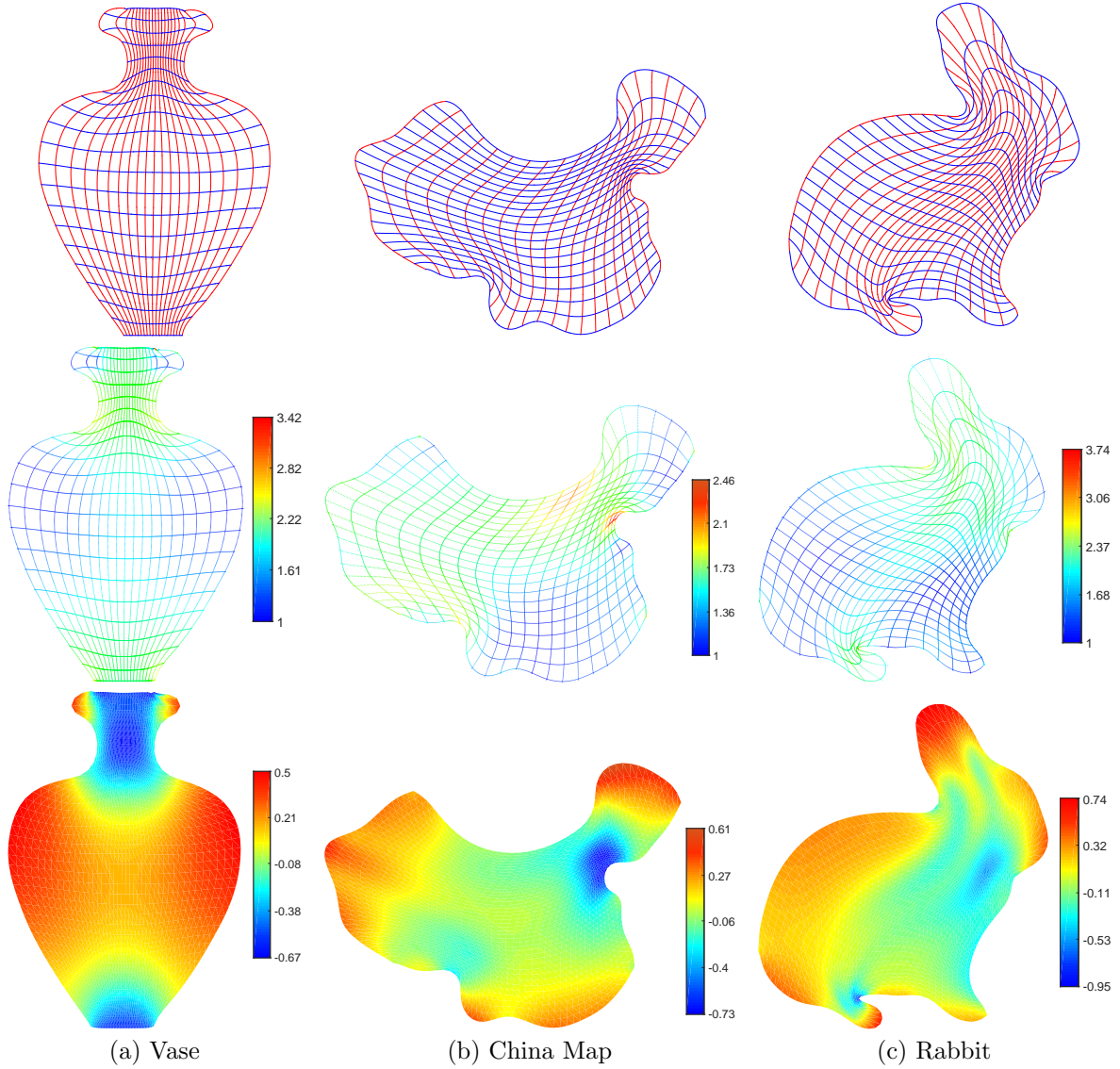


Figure 3: Parameterization of the vase, China Map and rabbit shaped domain by our method. The first row shows the isoparametric curves of the parameterization, the second row presents the colormaps of $\log_2 \kappa(J_f)$, and the last row depicts the colormaps of $\log_{10} J_f^s$. Note that the optimal value of $\log_{10} J_f^s$ is 0.

4. Application in solving PDEs with IGA

In this subsection, we apply our parameterization together with IGA to solve numerical partial differential equations (PDEs) on different domains. The stability and accuracy of the numerical simulation are compared with Xu's method [3] and the T-Map method.

Consider the following elliptic problem

$$\begin{cases} -\Delta u + u = \hat{f} & \text{in } \Omega \\ u|_{\partial\Omega} = g & \text{on } \partial\Omega \end{cases} \quad (14)$$

where $\hat{f}, g \in L^2(\Omega)$ are given. The variational form of the problem (14) consists in finding $u \in V = \{u|u \in H^1(\Omega), u|_{\partial\Omega} = g\}$, such that

$$a(u, v) = \hat{f}(v), \quad \forall v \in H_0^1(\Omega). \quad (15)$$

where

$$a(u, v) = \int_{\Omega} (\nabla u \cdot \nabla v + uv) dx dy, \quad \hat{f}(v) = \int_{\Omega} \hat{f} v dx dy$$

Let $u = w + g$, then the problem (15) is equivalent to find $w \in H_0^1(\Omega)$, such that

$$a(w, v) = l(v), \quad \forall v \in H_0^1(\Omega). \quad (16)$$

where $l(v) = \hat{f}(v) - a(g, v)$.

In the setting of isogeometric analysis, the domain Ω is parameterized by a global map $f : \hat{\Omega} \rightarrow \Omega$. The isogeometric discretization takes advantages of the given parameterization of the domain Ω . In particular, the discretization space V_h can be chosen as

$$V_h = \text{span}\{\phi_{ij}(x, y), i = 0, 1, \dots, m, j = 0, 1, \dots, n\}$$

with $\phi_{ij} = B_{ij} \circ f^{-1}(x, y)$ and $B_{ij}(\xi, \eta) = N_i^p(\xi)N_j^q(\eta)$.

The finite-dimensional space V_h is now used for the Galerkin discretization of the variational formulation (16), which consists in finding $w_h \in V_h$, such that

$$a(w_h, v_h) = l(v_h), \quad \forall v_h \in V_h. \quad (17)$$

We solve the above elliptic problem over two domain examples to show the numerical advantages of our new parameterization method. In the first example, we solve the elliptic problem over the bird-shaped domain, where u has an exact solution $\tanh((0.25 - \sqrt{(x - 0.5)^2 + (y - 0.5)^2})/0.03)$. The parameterization results of this domain are shown in the paper. And the degrees of freedom (DOF) of the basis functions in V_h in this example is 4225. Fig. 4(a), 4(b) and 4(c) show the numerical errors of the solutions for Xu's method, the T-Map method and our method respectively, and Table 2 summaries the condition numbers of the stiffness matrices and L_2 errors for these three methods. We can see that our method produces smaller condition numbers and errors than the other two methods, which is owing to the higher quality of our parameterization.

In the second example, we consider the elliptic problem (14) over another domain—the cow-shaped domain, whose parameterization results are shown in the paper. The DOF of the basis functions in V_h and the exact solution in this example are 16641 and $1.0/((x - 0.5)^2 + (y - 0.5)^2 + 0.02)$ respectively. Fig. 5(a), 5(b) and 5(c) show the numerical errors of the solutions and Table 3 lists the condition numbers of the stiffness matrices and L_2 errors for these three methods. Again we can see that our method produces smaller condition numbers and errors than the other two methods.

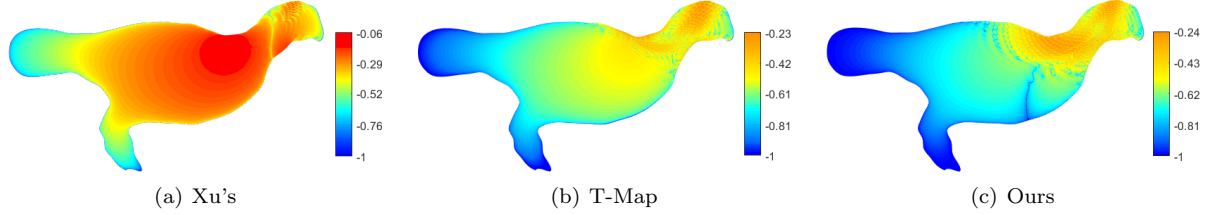


Figure 4: The errors in numerical solutions for different methods: (a) Xu’s method, (b) T-Map method and (c) Our method. Here for the ease of display, we plot the colormaps of $\frac{\log_{10}(|u-u_h|+1e-10)}{10}$.

	DOF	1089	4225	16641	66049
Xu’s	Condition number	1.28e+05	1.68e+05	4.22e+06	5.00e+06
	L_2 error	1.34e-02	1.48e-02	1.05e-02	1.57e-03
T-Map	Condition number	8.79e+03	3.80e+04	3.07e+05	3.41e+06
	L_2 error	5.04e-03	2.36e-04	6.83e-05	2.57e-06
Ours	Condition number	5.67e+03	1.51e+04	1.70e+05	3.36e+05
	L_2 error	2.59e-03	1.03e-04	4.49e-06	2.19e-07

Table 2: Comparisons of the condition numbers of the stiffness matrices and L_2 errors for the bird-shaped domain.

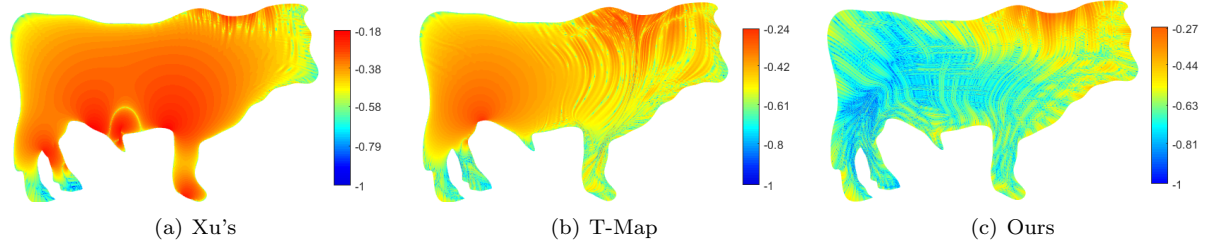


Figure 5: The errors in numerical solutions for different methods: (a) Xu’s method, (b) T-Map method and (c) Our method. Here for the ease of display, we plot the colormaps of $\frac{\log_{10}(|u-u_h|+1e-10)}{10}$.

	DOF	1089	4225	16641	66049
Xu’s	Condition number	6.20e+04	2.74e+05	8.38e+06	8.66e+07
	L_2 error	2.84e-02	1.33e-03	1.22e-03	1.06e-03
T-Map	Condition number	2.48e+04	6.62e+04	3.04e+05	6.37e+06
	L_2 error	6.49e-02	1.04e-03	2.28e-04	1.96e-04
Ours	Condition number	4.66e+03	1.80e+04	7.03e+04	2.77e+05
	L_2 error	2.97e-02	8.21e-04	7.94e-05	6.27e-06

Table 3: Comparisons of the condition numbers of the stiffness matrices and L_2 errors for the cow-shaped domain.

References

- [1] Maodong Pan, Yinlei Hu, and Yuanpeng Zhu. A Spline Representation for Planar Domains Based on Quasi-conformal Mapping. 2019.
- [2] Xianshun Nian and Falai Chen. Planar domain parameterization for isogeometric analysis based on teichmüller mapping. *Computer Methods in Applied Mechanics and Engineering*, 311:41–55, 2016.
- [3] Gang Xu, Bernard Mourrain, Régis Duvigneau, and André Galligo. Parameterization of computational domain in isogeometric analysis: methods and comparison. *Computer Methods in Applied Mechanics and Engineering*, 200(23):2021–2031, 2011.
- [4] Michael JD Powell. On search directions for minimization algorithms. *Mathematical programming*, 4(1):193–201, 1973.
- [5] Ka Chun Lam and Lok Ming Lui. Landmark-and intensity-based registration with large deformations via quasi-conformal maps. *SIAM Journal on Imaging Sciences*, 7(4):2364–2392, 2014.